Hindawi
Journal of Sensors
Volume 2022, Article ID 2216581, 13 pages
https://doi.org/10.1155/2022/2216581

Research Article

Intelligent Management of Land Resources Based on Internet of Things and GIS Technology

Hao Gong[1] and Chen He[2]

[1]*School of Land Science & Technology, China University of Geosciences (Beijing), Beijing 100083, China*
[2]*Faculty of Accounting, Hubei University of Economics, Wuhan 430205, China*

Correspondence should be addressed to Chen He; 00001678@hbue.edu.cn

Received 17 March 2022; Revised 13 April 2022; Accepted 19 April 2022; Published 11 May 2022

Academic Editor: Wen Zeng

In order to improve the effect of land resource management, this paper combines the Internet of Things technology and GIS technology to build an intelligent management system for gradient resources to improve the efficiency of land resource management. Aiming at the hybrid intelligent model of wetland resource remote sensing monitoring technology, this paper analyzes and studies the remote sensing image processing theory. Moreover, this paper studies in detail remote sensing image restoration, TM image reflectivity simulation imaging, image enhancement technology, optimal band selection based on the characteristics of wetland resources, expert decision analysis, deep mining of image data, knowledge reasoning, and decision tree analysis to form a theoretical support system for a hybrid intelligent classification model for wetland resources. The research shows that the intelligent management system of land resources based on the Internet of Things and GIS technology has a good effect in the collection and processing of land resource information and can effectively improve the management efficiency of land resources.

1. Introduction

China has a vast territory and abundant resources in absolute quantity, but the per capita quantity is insufficient. Moreover, the natural resources, ecological and environmental conditions, and social and economic development vary greatly from place to place, and the stages of development and the problems existing in the development are also different. If we do not consider the characteristics and differences of regions and use the same standard to measure the development of various regions, it will be difficult for the evaluation to be objective and fair. At the same time, when the same policy is used to guide the development of various regions, the measures are often lacking in pertinence and effectiveness. In addition, with the rapid increase of the population, on the one hand, the area of arable land in China has dropped sharply, the land has been degraded, and the land reserve resources are seriously insufficient. On the other hand, extensive land use, low utilization rate, and low output rate make the situation of land resources increasingly severe and the contradiction between man and land increasingly prominent.

The research on comprehensive land carrying capacity has its own characteristics: first, the research on comprehensive land carrying capacity is a systematic perspective on regional land, grain, population, and social development. It involves many aspects and is affected by many factors, of which nature and humanity are the two most important ones. Natural factors include the quantity and quality of land resources, regional climatic conditions and water resources, etc.; human factors include population status, the level of social and economic development, the rationality of technological level resource utilization, etc. These factors together affect the level of carrying capacity of land resources makes it an intricate system. Secondly, while the research on comprehensive land carrying capacity has been improved with the development of science and technology and some natural processes, it does not mean that it can develop permanently and unrestrictedly. It is constrained by two aspects: the absolute limit of the productivity of land resources and

the relative limit over a certain period of time. The former refers to the ultimate source of productivity of land resources—solar radiation energy is limited per unit area; especially, the conversion rate of solar energy cannot exceed a certain limit, thus stipulating the limit of productivity of land resources. In the foreseeable future, it is impossible for the development of science and technology to break through the limit of land productivity, such as the level of grain yield per unit. The limit of land production capacity determines the limit of land carrying capacity, which has far-reaching significance for objectively grasping the regional resource-population problem.

The "comprehensive" study of comprehensive land carrying capacity includes two meanings [1]. On the one hand, for the carrier, the land should not be limited to cultivated land but should be a generalized land including garden land, forest land, pasture land, urban settlements and industrial and mining land, water area, transportation land, and unused land. On the other hand is the question of what to carry, that is, carrying substance. Land problems are caused by human social and economic activities. The goal of land use is to coordinate human social and economic activities with the corresponding environment and to protect and improve the land resources for human survival and development. Therefore, the bearing object should be various social and economic activities of human beings, such as the city scale, economic output value, transportation scale, land pollution capacity, etc., not only the bearing population size and population consumption pressure, which forms the "comprehensive carrying capacity of land." The comprehensive carrying capacity of land refers to the maximum population and urban development scale that the land resources can bear on the basis of the foreseeable level of technological, economic and social development, the principle of sustainable development, and the premise of maintaining the benign development of the human ecological environment under the current development stage [2]. That is to say, the size of the comprehensive land carrying capacity is not only a reflection of the characteristics of the natural geographical environment but also depends on the development level of human society, economy, and technology; the effective use of land resources by humans; and the improvement of the ecological environment [3].

This paper combines the Internet of Things technology and GIS technology to build an intelligent management system for gradient resources, improve the efficiency of land resource management, and effectively promote the progress and development of intelligent land management technology.

2. Related Work

Literature [4] establishes a real estate database management system, which integrates the decentralized management of land registers and other information, which greatly improves work efficiency; in the application research of basic farmland management information system, literature [5] uses MapGIS secondary. The development library SDK builds a permanent basic farmland database and uses C++ language to design and implement a basic farmland demarcation system. Based on the MapGISK9 platform, Yang Weibin of Xiamen University adopts a combination of C/S and B/S architecture to solve the possible defects of the basic farmland management information system. Literature [6] developed the basic farmland management information system of Ninghua County based on ArcGIS Engine components and C# as the development language. Literature [7] used Oracle as the database management platform and ArcSDE as the spatial database search engine, participated in the design and establishment of the basic farmland management information system in Sichuan Province, and used ArcGIS Server server and WebService technology to enable the public to conduct related business queries on the browser side. These attempts in basic farmland information management have provided effective advanced experience for the system construction of farmland protection [8]. However, a large part of the region has not established a comprehensive and effective basic farmland information system, and we still need to explore and work together [9]. The use of UML language and CASE tools is the trend of GIS software development [10]. Literature [11] studies and summarizes the development process of cadastral information system by adopting the object-oriented GIS development method and combining with UML. Literature [12] describes the land change process realized by drawing lines with the mouse using UML and realizes the land change subsystem in the land management information system by means of secondary development. These studies reflect the application of UML technology in land information management software development from different angles and meet the needs of software system development in GIS projects. On the basis of the above practice, further research is carried out in combination with the characteristics of permanent basic farmland data and applications. The theoretical technology of geographic information system has gone through the process of desktop geographic information system, client/server mode in local area network, and WebGIS [13]. At present, the land information system is still in the stage of continuous development and generally shows the following development trends: (1) The integration with remote sensing system (RS), global positioning system (GPS), and other technologies needs to be strengthened. Surveying and mapping technologies such as RS and GPS can provide strong technical support for the real-time collection of large-area land use information and achieve high precision and automation of ground data collection [14]. (2) Modern land management information systems not only care about the distribution area, and it is a research direction of land management information system [15]. (3) With the help of artificial intelligence theory and expert system technology enables computers to use expert knowledge to simulate human brain thinking for reasoning, which can greatly improve work efficiency, and its applications in cartography, spatial decision support, and intelligent data processing need to be further deepened [16]. (4) With the advent of the era of big data and the rapid development of network technology, the use of the Internet to publish spatial data and provide users with the functions of spatial data browsing, query, and making thematic maps and analysis has become an inevitable trend in the development of land information systems [17]. Literature [18] proposes to build a "land and resources cloud"

technology system and create an "Internet + land and resources service" model, which is to make full use of advanced concepts and technologies such as cloud computing and big data to achieve unified deployment of services and comprehensive data sharing.

3. Remote Sensing Image Processing Based on Internet of Things and GIS

After the GCP ground control point selection is completed, the pixel coordinates (x, y) should be converted into image coordinates that are related to the reference coordinates (X, Y) through a mathematical model. The selected coordinate change function (mathematical correction model) is a polynomial correction model, and commonly used image correction functions include polynomial, Legendre polynomial, and collinear correction. Because the polynomial principle is intuitive, the calculation is simple, and it has better accuracy; the polynomial correction method is generally chosen. In this study, a quadratic polynomial function is used to perform precise geometric correction. The formula is as follows:

$$\begin{aligned} x &= a_0 + a_1X + a_2Y + a_3X^2 + a_4XY + a_5Y^2, \\ y &= b_0 + b_1X + b_2Y + b_3X^2 + b_4XY + b_5Y^2. \end{aligned} \tag{1}$$

Polynomial coefficients (conversion parameters) are obtained by least squares regression. According to the root mean square error formula ($\mathrm{RMS}_{\mathrm{error}}$), the difference between the estimated coordinates and the original coordinates is obtained.

$$\mathrm{RMS}_{\mathrm{error}} = \sqrt{\left(x' - x\right)^2 + \left(y' - y\right)^2}, \tag{2}$$

That is, by calculating the root mean square error of each control point, the ground control points with larger errors can be checked, and the accumulated overall root mean square error can be obtained, so as to obtain the accuracy of coordinate change.

The absorptivity and reflectivity of an object vary with the temperature of the object and the wavelength of incident radiant energy, so we define the monochromatic reflectance and monochromatic absorptivity of an object as [19]:

$$\alpha(\lambda) = \frac{E_\alpha(\lambda)}{E}, \tag{3}$$

$$\rho(\lambda) = \frac{E_r(\lambda)}{E}. \tag{4}$$

In the formula, $a(\lambda)$ is the monochromatic absorptivity of light with wavelength λ, $\rho(\lambda)$ is the monochromatic reflectance of light with wavelength λ, $E_a(\lambda)$ is the energy absorbed by light with wavelength λ incident on the surface of an opaque object, $E_r(\lambda)$ is the energy reflected by the light with wavelength λ incident on the surface of an opaque object, and E is the total incident energy.

We use the TM data to make the principle of simulated reflectivity image, and the energy carried by the color light of different bands and the weight W_i of the total energy are shown in the table. From this, we can obtain the total reflected energy:

$$E\rho = \sum_{i=1}^{5} W_i TM_i + W_7 TM_7. \tag{5}$$

In the formula, $E\rho$ is the total reflected energy, K_i is the weight of the i-th band in the total energy, TM_l is the remote sensing data of the i-th band, W_7 is the weight of the seventh band in the total energy, and TM_7 is the remote sensing data of the seventh band.

From Wien's displacement theorem λ max = 2897/T, it can be known that with the increase of temperature, the peak value of radiant emission shifts to the short-wave direction. When the surface temperature is -60°C, the wavelength peak of the surface radiation is 13.6 μm, and when the surface temperature is 60°C, the wavelength peak of the surface radiation is 8.7 μm. The surface temperature is generally between -60°C and 60°C, and the radiated wavelength peak falls within the wavelength range of TM6. Therefore, the relative value of the energy lost by the earth due to long-wave radiation can be represented by TM6.

The surface of the earth with the size of each pixel receives the light energy of the sun as E_0, then:

$$E = E_a + E_p, \tag{6}$$

$$a + p = 1. \tag{7}$$

The energy change of a pixel on the earth's surface (expressed as a temperature difference change) is E_Δ, and the scattered energy is E_e, then:

$$E_\Delta = E - E_e - E_p. \tag{8}$$

That is,

$$E - E_\Delta = E_e + E_\rho. \tag{9}$$

Since the relative value of the energy lost by the earth due to long-wave radiation can be represented by TM_6, formula (7) can be written as follows:

$$E - E_\Delta = TM_6 + E_\rho. \tag{10}$$

We set:

$$P_{\mathrm{sim}}(\lambda) = \frac{E_r(\lambda)}{E - E_\Delta} = \frac{E_r(\lambda)}{TM_6 + E_\rho}. \tag{11}$$

In a very small time, the temperature difference change of the surface can be ignored; that is, $E_\Delta = 0$, and formula (9) can be transformed into:

$$P_{\text{sim}}(\lambda) = \frac{E_r(\lambda)}{E} = \frac{E_r(\lambda)}{E_{tm_6} + E_\rho}. \quad (12)$$

Since E_Δ is not strictly equal to 0, we call P_{sin} as the monochromatic reflectance. Through the different energy values of different bands, the monochromatic reflectance data of each band in the TM band can be obtained, and the synthesized color map is called the simulated reflectance map.

The first step in band combination is to select a band by numerical evaluation according to the amount of information contained in each band of a remote sensing image. Through analysis, it can be determined which parts or which bands (i.e., band subsets) contain the amount of information. The standard deviation of each band reflects the total dispersion of the gray value and the average value of each pixel in the image and to a certain extent reflects the amount of information in each band. The larger the value, the greater the amount of information contained. The amount of ground object information contained in each band of a TM image is generally measured by the radiation quantization level covered by the band image, that is, the range of brightness values or brightness difference (maximum brightness value-minimum brightness value).

The standard deviation formula is

$$S = \frac{1}{MN}\sqrt{\sum_m \sum_n \left(A_{ij} - A_0\right)}. \quad (13)$$

An image is A_{ij}, $(i = 1, 2, 3\cdots\cdots; j = 1, 2, 3\cdots\cdots)$, its image matrix size is $M \times N$, and $A_o$represents the average gray value of the whole image. The brightness difference reflects the degree of change in the gray value, and its magnitude is equal to the maximum brightness value minus the minimum brightness value, and the formula is $f\text{range}(i, j) = f\ \max(i, j) - f\ \min(i, j)$. The mean vector represents the average reflection intensity of the objects in the image.

$$f = \frac{\sum_{i=0}^{M-1}\sum_{j=0}^{N-1} f(i, j)}{MN}. \quad (14)$$

The correlation coefficient between the bands reflects the degree of information overlap between the two bands. If the correlation coefficient between the two bands is large, it means that their information overlap is high. Therefore, two channels with high correlation can be combined into one or one of the channels can be taken as one. The formula for the correlation coefficient between the bands is as follows:

$$R = \frac{S_{ij}^2}{S_{ij}S_j}. \quad (15)$$

In the formula, $S_{ij} = \text{COV}(i, j) = (1/N)\sum_{k=1}^{n}(Xik - \overline{Xi})(Y_{jk}\overline{Y_j})$.

Among them,*i*, *j*is the number of bands 1, 2, 3, 4, 5, and 7, and$S_{ij}$is the covariance between the*i*-th band and the*j*-th band,$\bar{x}i$is the spectral gray mean value of the*i*-th band,$\bar{x}$is the gray value of the*k*-th pixel in the*i*-th band, and$Y_{jk}$is the gray-scale value of the*k*-th pixel in the*j*-th band.$\bar{Y}_j$ is the spectral gray mean value of the *j*-th band; $k = 1, 2, 3\cdots\cdots, n$ is the number of pixels in the experimental sample area. The larger the *R*, the greater the information overlap between the bands. The calculation of the band correlation coefficient matrix is relatively simple, and the general image processing software has this function. The analysis of the correlation coefficient becomes the basis of the band selection, and the calculation of the correlation coefficient is also necessary for the optimal index method.

Because the larger the standard deviation of the image data, the larger the amount of information it contains, and the smaller the correlation coefficient between the bands, which indicates that the independence of the image data in each band is higher and the information redundancy is smaller. Therefore, the concept of the optimal index (OIF) proposed by Chavez in the United States can also be used.

$$\text{OIF} = \frac{\sum_{i=1}^{3} S_l}{\sum_{r=1}^{3} Ri_j}. \quad (16)$$

Among them,$S_i$is the standard deviation of the*i*-th band, and$S_{ij}$is the correlation coefficient of the*i*and*j*bands. The larger the OIF, the greater the information content of the corresponding combined image. The OIF values are arranged from large to small, and the band corresponding to the largest OIF value is the best band combination. This method is currently the most commonly used band selection method. Moreover, the calculation method is simple, easy to operate, and closer to the principle of band selection.

The joint entropy represents the information amount of the combination of multiple bands, and the combined band with the largest joint entropy is the best band in the sense of "the largest amount of information." However, the joint entropy method requires a considerable amount of calculation and is generally not easy to operate. When computing, we need to write a program to implement it.

The entropy of an 8bit image *X* is

$$H(x) = -\sum_{i=0}^{255} p_i \log p_i\,(\text{Bit}). \quad (17)$$

In the formula, p_i is the probability that the gray value of the image pixel is *i*. Similarly, the joint entropy of 2-3 images is as follows:

$$\begin{aligned} H(x_1, x_2) &= -\sum_{i_1, i_2=0}^{255} p_{i_1} p_{i_2} \log p_{i,i_2}, \\ H(x_1, x_2, x_3) &= -\sum_{i1,i,i,3=0}^{255} p_{i,l_3,} \cdot \log p_{i,i_2 i_3}. \end{aligned} \quad (18)$$

In the formula,P_{i1}, P_{i2}, P_{i3}represents that the gray value of the pixel in the image$X_1$is*i*1; the gray value of the pixel with the same name in the image$X_2$is*i*2, and the gray value of the pixel with the same name in the image$X_3$is the joint

probability of$i3$. Generally speaking, the larger$H(x)$ and$H(x_1, x_2, x_3)$, the richer the information contained in the image (or group of images). Using entropy and joint entropy, bands and band combinations with a large amount of information can be obtained.

The learning process of BP algorithm consists of two aspects: forward propagation and back propagation. In the forward propagation process, the input pattern is processed layer by layer from the input layer through the hidden layer and finally transmitted to the output layer. The output state of each layer of neurons only affects the input state of the next layer of neurons. If the expected output cannot be obtained in the output layer, backpropagation is performed, the error signal is returned along the original path, and the weights and thresholds between neurons in each layer are corrected to make the error meet the requirements. For the BP algorithm, the commonly used network error is the mean square error function, which is defined as follows:

$$E_p = \frac{1}{2}\sum_{j=1}^{N}\left(t_{pj} - o_{pj}\right)^2. \tag{19}$$

Among them, E_p is the error of the p-th network vector, t_{pj} is the expected value of the j-th output neuron, and o_{pj} is the actual value of the j-th output neuron.

The central idea of the BP algorithm is to adjust the weights to minimize the total error of the network; that is, the mean square error E_p between the expected value and the output value of the neural network tends to be the smallest. The negative gradient of the error function of the weights points in the direction in which the error function decreases the fastest. If the algorithm moves along this vector in the weight space, it will eventually reach a minimum, at which point the gradient is zero. The weight adjustment formula is mathematically described as follows:

$$\Delta_p W_{ji} \infty - \frac{\partial E_p}{\partial w_{ji}}. \tag{20}$$

In the formula, $\triangle_P W_{ji}$ represents the change of the weight between the source neuron i in the $L-1$ layer and the destination neuron j in the L layer. This change in the weights causes the gradient to change in the direction of reducing the error in the weight space.

The goal of the entire BP algorithm is to determine how to adjust each weight to make the network converge. Formula (3) describes the relationship that each weight w_{ij} will change in the direction of the negative gradient where the local error decreases most rapidly. Converting it into an expression suitable for computer implementation, the differential equation required by the BP algorithm can be obtained:

$$\Delta_p w_{jt} = \eta \delta_{pj} O_{pi}. \tag{21}$$

In the formula, η is the learning rate, δ_{pj} is the error signal of the neuron j in the L layer, and 0_{pj} is the output of the neuron i in the $L-1$ layer.

The error signal can be expressed as follows:

For output neurons: $\delta_{pj} = (t_{pj} - O_{pj})O_{pj}(1 - O_{pj})$.

For hidden layer neurons: $\delta_{pj} = O_{pj}(1 - O_{pj})\sum_k \delta_{pk}\omega_{ij}$.

In the formula, O_{pj} represents the output of neuron j in layer L, O_{pi} represents the output of neuron i in layer $L-1$, and δ_{pk} represents the error signal of neuron k in layer $L+1$.

According to the above description, the whole BP learning algorithm can be described as follows:

(1) The algorithm randomly gives the input layer unit to the hidden layer unit, the hidden layer unit to the output layer unit, the threshold value of the hidden layer unit, and the threshold value of the output layer unit. Generally, a small random number within (-1, +1) is assigned

(2) The algorithm performs the following operations on $(x_k, y_k)(k = 1, 2, \cdots m)$ for the sample pattern

(2-1) The algorithm sends the value of x_k to the input layer unit and calculates the new activation value of the hidden layer unit of the network.

$$O_{pj}^{(1)} = f_j\left(\text{net}_{pj}^{(1)}\right) j = 1, 2, \cdots, M. \tag{22}$$

(2-2) The algorithm calculates the activation value of the output layer unit.

$$O_{pj}^{(2)} = f_j\left(\text{net}_{pj}^{(2)}\right) j = 1, 2, \cdots, N. \tag{23}$$

(2-3) The algorithm calculates the output layer unit and the generalization error.

$$\delta_{pj}^{(2)} = O_{pj}^{(2)}\left(1 - O_{pj}^{(2)}\right)\left(t_{pj} - O_{pj}^{(2)}\right) j = 1, 2, \cdots, N. \tag{24}$$

(2-4) The algorithm calculates the training error of the hidden layer unit.

$$\delta_{pj}^{(1)} = O_{pj}^{(1)}\left(1 - O_{pj}^{(1)}\right)\sum_{k=1}^{N}\delta_{pk}^{(2)}\omega_{kj}^{(2)} j = 1, 2, \cdots, M. \tag{25}$$

(2-5) The algorithm adjusts the connection weight from the hidden layer to the output layer.

$\Delta w_{ij} = \eta {O_{pj}}^{(1)}{\delta_{pj}}^{(2)}\eta$ is the learning rate, $0 < \eta < 1$.

(2-6) The algorithm adjusts the connection weight from the input layer to the hidden layer.

$$\Delta w_{kj} = \eta A_k \delta_{pj}^{(1)}. \tag{26}$$

(2-7) The algorithm adjusts the threshold from the output layer to the hidden layer.

$$\Delta r_j = \eta \delta_{pj}^{(2)}. \tag{27}$$

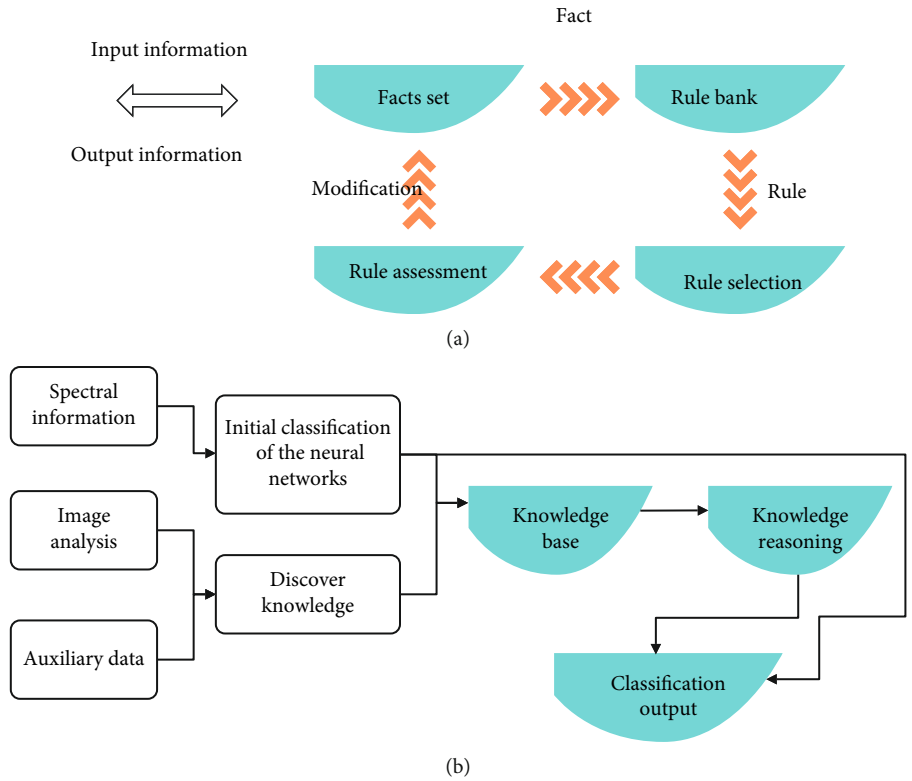

Figure 1: Data flow and basic idea of hybrid AI system: (a) data flow in the rules; (b) rule discovery.

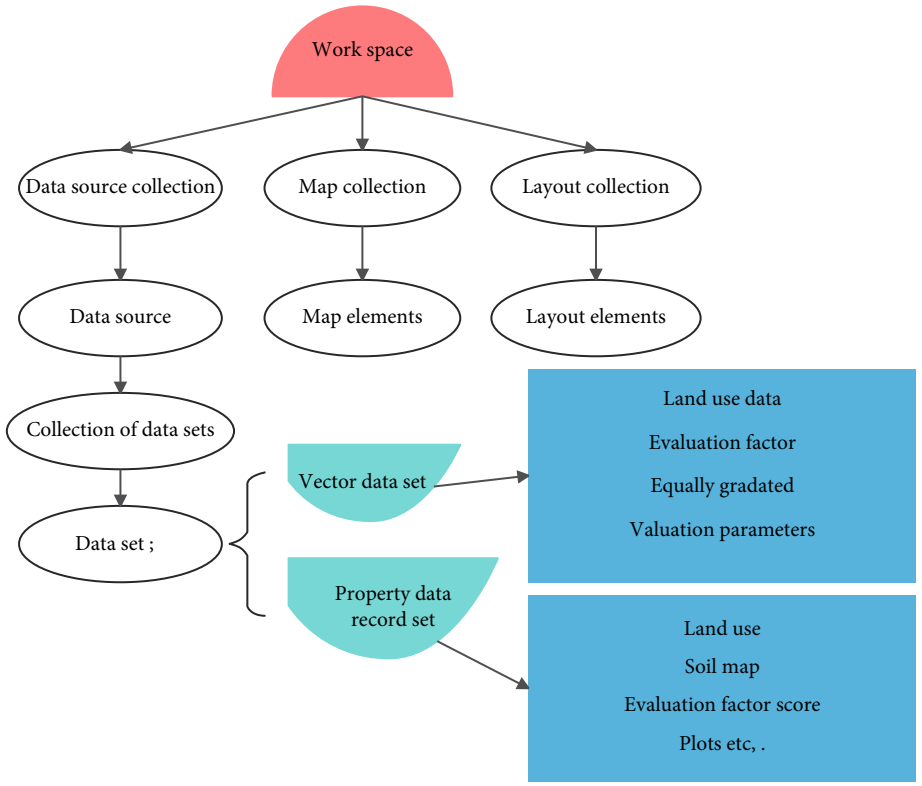

Figure 2: The structure frame of the data mining library.

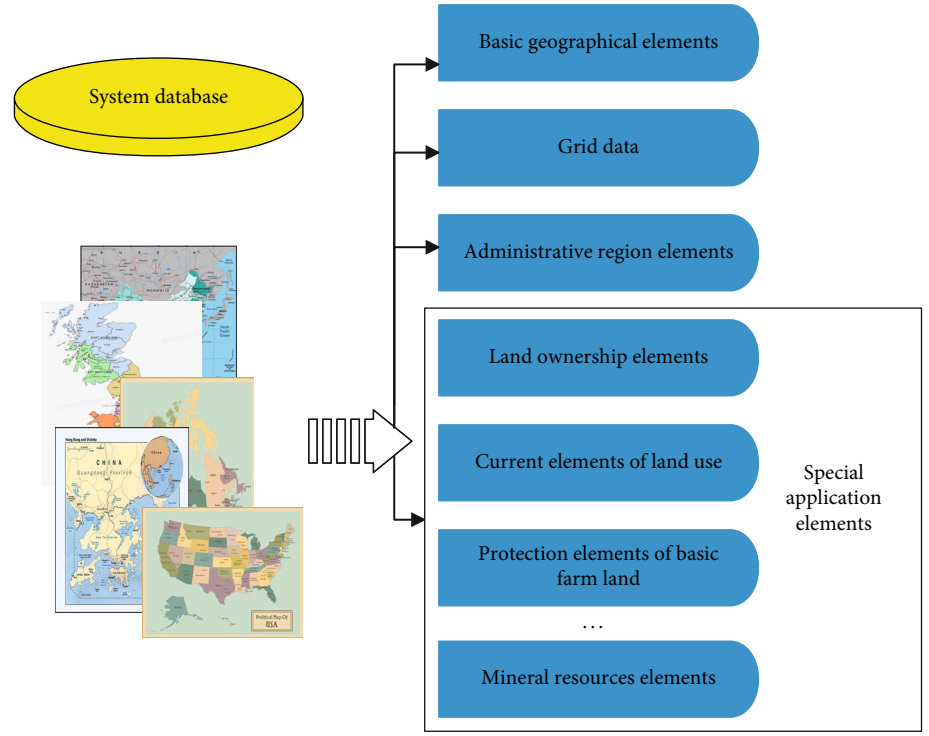

Figure 3: System data frame.

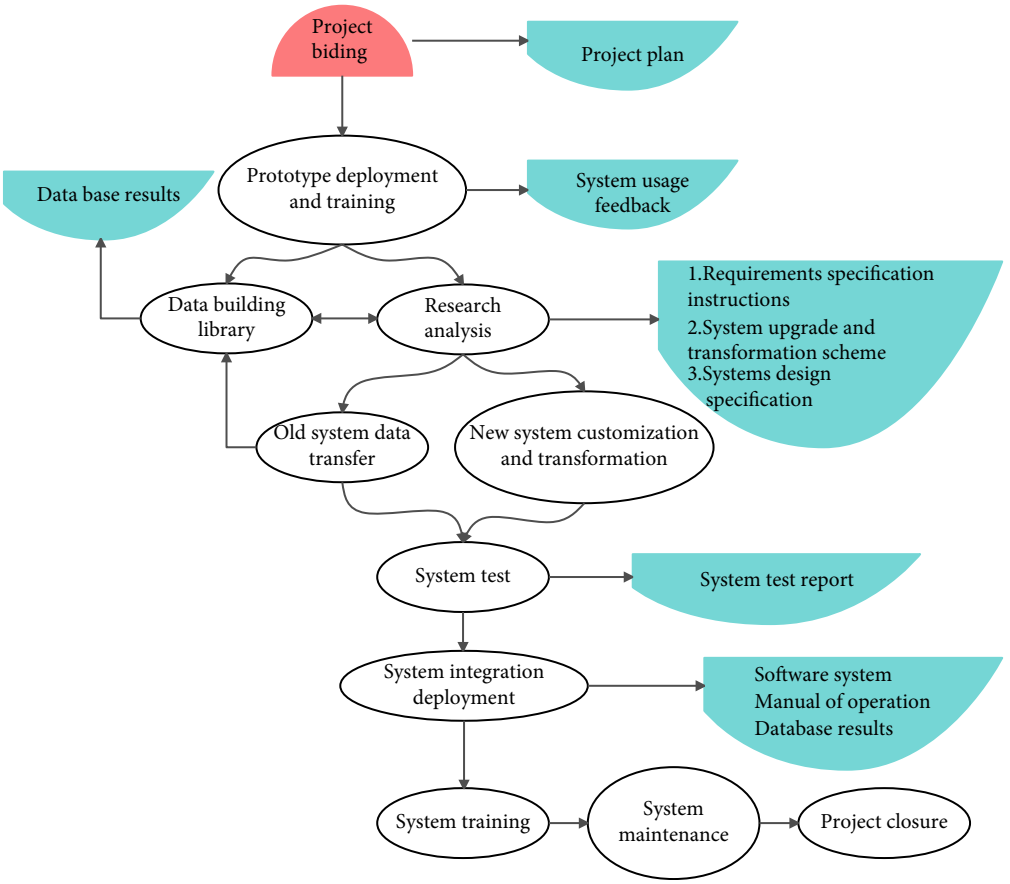

Figure 4: Implementation of the system.

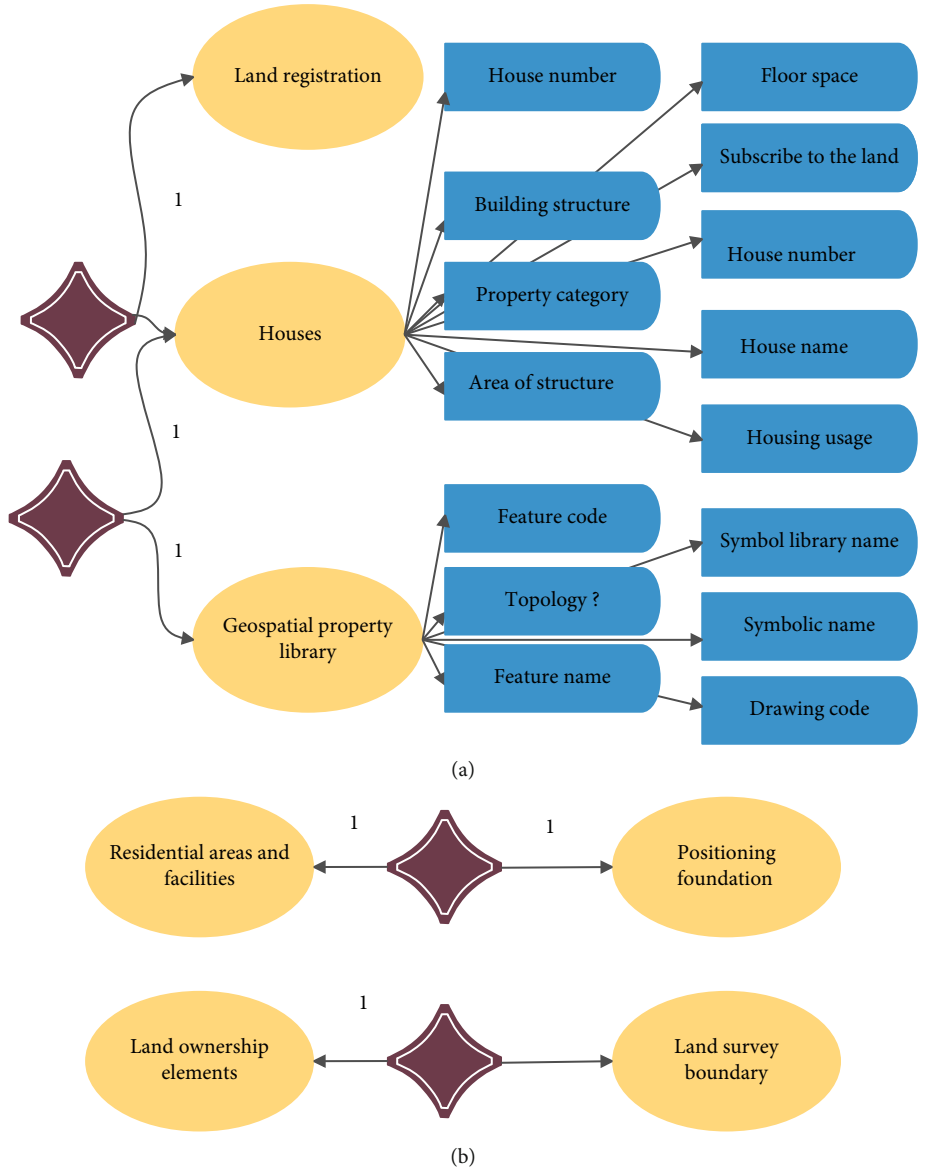

Figure 5: The design of the database E-R mode: (a) ER model of land registry business; (b) ER model of the underlying geography.

(2-8) The algorithm adjusts the threshold of the hidden layer unit.

$$\Delta\theta_j = \eta\delta_{pj}^{(1)}. \tag{28}$$

(3) The algorithm judges whether the error meets the requirements. If the requirements are satisfied, the algorithm executes step 5, otherwise, executes step 4

(4) The algorithm judges whether the maximum number of iterations is exceeded. If it exceeds, it means that the training fails, and step 5 is performed; otherwise, it returns to step 2

(5) The algorithm ends

The shape and size of a feature is one of the important signs to identify a feature. The description of the shape includes regular geometric shapes, such as rectangle, square, rhombus, diagonal, circle, ellipse, and pentagon, as well as some irregular geometric figures. The shape soil of the measurement object is the perimeter P and area A of the base-inch object, and its shape index K is defined as follows:

$$K = \sqrt{\frac{A}{P}}. \tag{29}$$

The shapes of various types of objects are summarized into the following types.

3.1. Round. For areas of equal area, a circle has the shortest perimeter, and an object that has the shape of a circle will have the largest area/perimeter ratio. For any circular object, it is not difficult to derive the following relationship:

$$\sqrt{\frac{A}{P}} = \frac{1}{2\sqrt{p}} > \frac{1}{4}. \tag{30}$$

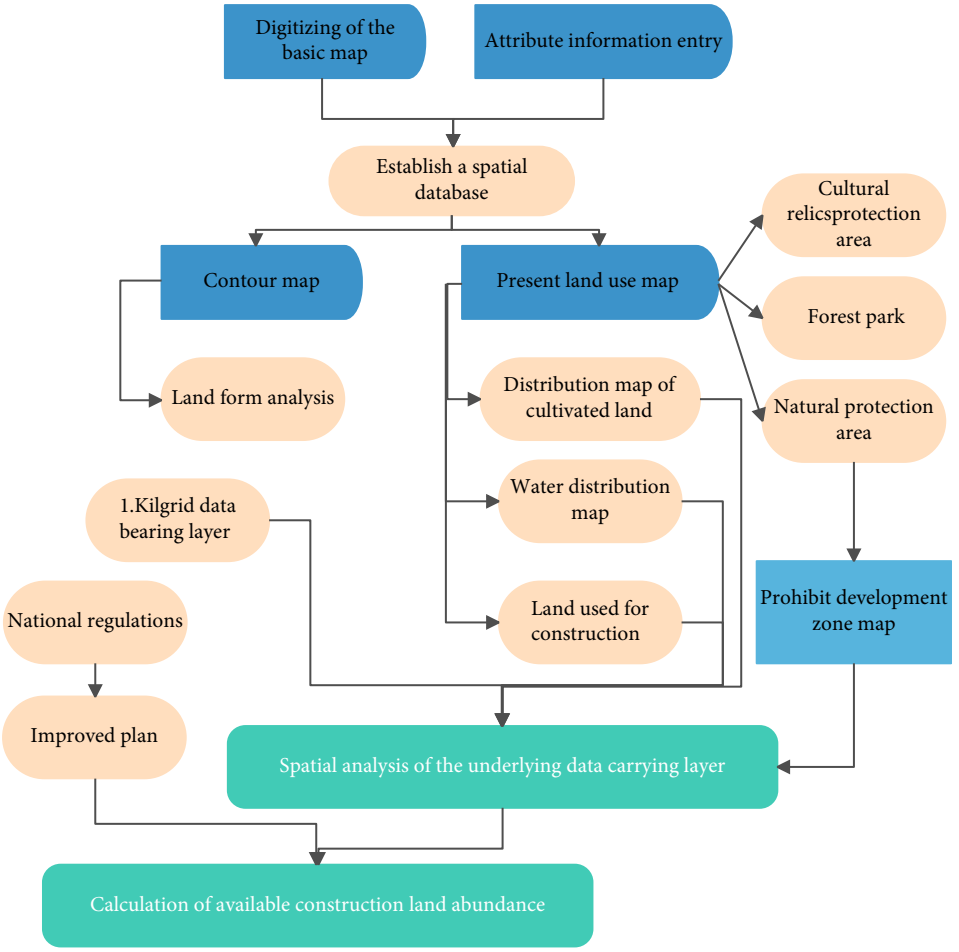

Figure 6: Basic work flow chart.

3.2. Square. Square objects can share the following relationships:

$$\sqrt{\frac{A}{P}} = \frac{1}{4}. \tag{31}$$

The shape index of a square is smaller than that of a circle.

3.3. Rectangle. If the long side of the rectangle is k times the short side, it can have the following relationship:

$$\sqrt{\frac{A}{P}} = \sqrt{\frac{k}{2}(k+1)} < \frac{1}{4}. \tag{32}$$

3.4. Linear Objects. Linear objects have small shape index values, and such objects include roads, rivers, and airports.

3.5. Irregular Objects. The more complex the shape of this type of object, the smaller its shape index. For some objects that share obvious shapes, it is the most effective method to use shape information to identify them. The shape index K can be used as an important indicator to measure the shape of an object. A complex or long object always has a smaller shape index value. Conversely, a simple or round object has a larger shape index value.

The area of an object can also be used as another important shape indicator to identify some different types of objects. For example, the shape index of a lake and a reservoir may be similar, but the area of a lake is much larger than that of a reservoir, and they can be completely distinguished based on the area index.

After the knowledge is expressed in an appropriate way, it is necessary to study the reasoning mechanism for using the knowledge. Reasoning is the thinking process of drawing a new judgment from a known judgment according to a given principle. In the remote sensing image knowledge inference system, rule inference and rule expression use production rules to describe the solution to the problem. This kind of rule-based inference is also called production inference. At the same time, roughly speaking, production reasoning is the reasoning engine selects the rules from the rule base and applies the rules. When these selected rules are applied, they perform the actions of the concluding part of the rules and thus lead to the addition, deletion, modification, etc. of the

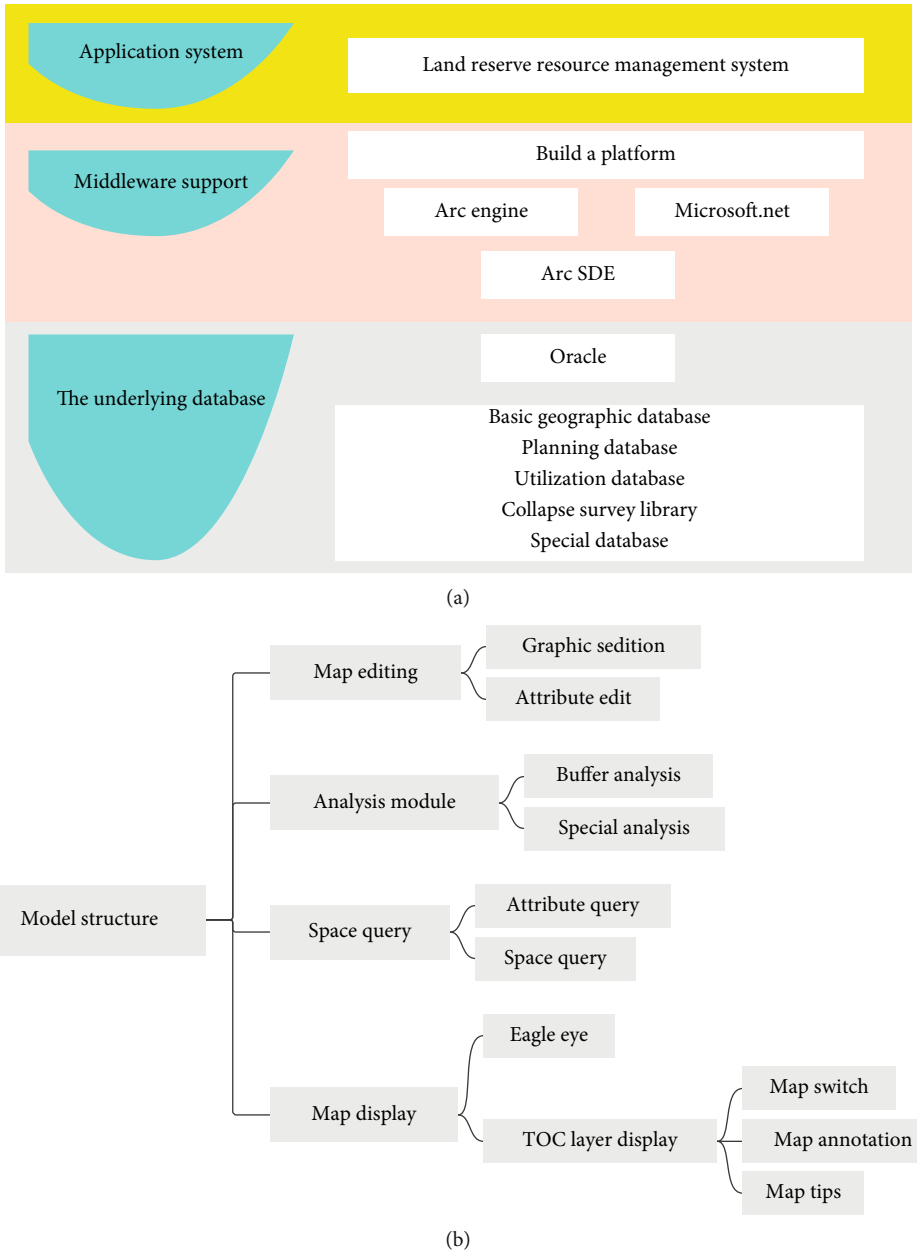

Figure 7: Intelligent management system of land resources based on Internet of Things and GIS technology: (a) structure diagram of land reserve resource management system; (b) schematic diagram of the overall structure of the frame.

facts in the fact base. Figure 1(a) is a schematic diagram of the changes of rules and facts in the working process of the inference engine, and the direction of the arrow indicates the direction of data flow. Figure 1(b) is the rule discovery.

In the object-oriented knowledge representation, the operation of the object is contained in the object; that is, the reasoning is distributed in each object. Rules represent the way and strategy of reasoning and are used to represent the experience of experts in the specific application of knowledge. During inference, when the fact expression is consistent with the conditional expression of the rule in the knowledge base, inference can be generated according to the rule, and the credibility value given by the expert can be obtained.

4. Intelligent Management of Land Resources Based on Internet of Things and GIS Technology

The design of the system database mainly adopts the top-down design scheme and the object-oriented programming idea. The top layer is the workspace, which includes three parts: data source set, map set, and layout set. Map set and layout set are mainly used for map output of spatial data, and they are composed of map elements and layout elements, respectively. Moreover, the data source set can derive subclass data source, the data source is composed of the data set, and the data set is a subclass of the data set, which

Table 1: The effect of intelligent treatment of land resources.

Number	Information processing	Number	Information processing	Number	Information processing	Number	Information processing
1	86.112	19	90.639	37	91.603	55	90.024
2	85.688	20	91.070	38	90.174	56	91.803
3	87.955	21	86.180	39	84.736	57	84.129
4	92.038	22	84.174	40	92.911	58	86.351
5	86.368	23	84.961	41	91.897	59	89.671
6	89.744	24	84.884	42	84.434	60	88.926
7	89.109	25	92.701	43	84.671	61	86.935
8	90.527	26	90.730	44	84.217	62	92.007
9	86.701	27	89.684	45	89.516	63	88.405
10	85.062	28	86.349	46	85.361	64	92.278
11	91.437	29	92.040	47	89.637	65	87.194
12	91.564	30	85.535	48	87.674	66	88.478
13	85.800	31	87.064	49	88.757	67	86.047
14	89.195	32	91.311	50	91.295	68	90.638
15	92.765	33	91.022	51	84.898	69	89.595
16	91.210	34	92.832	52	87.312	70	89.139
17	85.537	35	85.918	53	86.181	71	92.262
18	90.494	36	84.648	54	90.821	72	89.216

Table 2: The effect of land resource management.

Number	Land management	Number	Land management	Number	Land management	Number	Land management
1	83.101	19	82.675	37	81.887	55	83.482
2	80.579	20	83.033	38	86.298	56	80.108
3	81.242	21	80.846	39	85.034	57	80.538
4	87.008	22	83.737	40	83.202	58	82.808
5	85.425	23	84.360	41	80.487	59	83.085
6	86.776	24	83.579	42	82.218	60	86.631
7	86.118	25	85.664	43	81.450	61	85.964
8	81.128	26	80.772	44	81.636	62	85.311
9	86.674	27	85.902	45	85.149	63	82.297
10	83.050	28	84.112	46	82.483	64	85.543
11	84.867	29	87.334	47	80.371	65	82.051
12	86.532	30	81.800	48	83.378	66	85.295
13	81.277	31	84.093	49	83.510	67	81.233
14	80.343	32	81.997	50	83.546	68	81.354
15	82.522	33	85.829	51	86.196	69	87.817
16	86.037	34	80.677	52	83.581	70	87.873
17	81.763	35	82.276	53	82.413	71	81.881
18	82.962	36	82.831	54	81.405	72	81.550

includes the vector data set attribute data record set. Its structural frame is shown in Figure 2.

The data can be logically divided into spatial data, image data, attribute data, public configuration data, and document data. Spatial databases are divided into two categories. One is basic geographic data, administrative area data, and image data, which are provided to other applications as shared data. The other category is each thematic application elements as shown in Figure 3.

The implementation strategy that goes hand in hand with prototype trial, database building, and software customization and transformation is specified. The implementation scheme

of intelligent management of land resources based on the Internet of Things and GIS technology is shown in Figure 4.

The design of the database E-R model is shown in Figure 5, in which Figure 5(a) is the ER model of the land registration business, and Figure 5(b) is the basic geographic ER model.

The construction land resource evaluation study is based on the workflow shown in Figure 6.

This system uses the current land survey data, planning data, and agricultural special data as the analysis data; uses C# as the development front-end; and is designed and developed based on ArcGIS Engine. The system structure is shown in Figure 7(a), and the framework generally includes five parts: map display, query module, analysis module, and land evaluation, as shown in Figure 7(b).

On the basis of the above research, the intelligent management system of land resources based on the Internet of Things and GIS technology proposed in this paper is evaluated, and the effect of intelligent processing of land resources and the effect of land resource management are counted, and the results shown in Tables 1 and 2 are obtained.

From the above research, it can be seen that the intelligent land resource management system based on the Internet of Things and GIS technology has a good effect in the collection and processing of land resource information and can effectively improve the management efficiency of land resources.

5. Conclusion

According to the resource and environmental carrying capacity, existing development density, and development potential of different regions, this paper considers the future population distribution, economic layout, land use, and urbanization pattern and divides the land space into four main functional areas: optimized development, key development, restricted development, and prohibited development. Moreover, this paper clarifies the main function, guides the development direction, regulates the development order, controls the development intensity, adjusts the development policy, and gradually forms a new pattern of spatial development in which population, economy, resources, and environment are coordinated. The main functional area is the product of implementing the scientific concept of development, and the proposal of the main functional area plan is also a new breakthrough in promoting the coordinated development of the region, and it is the regional embodiment of the sustainable development strategy. This paper combines the Internet of Things technology and GIS technology to build an intelligent management system for gradient resources. The research shows that the intelligent management system of land resources based on the Internet of Things and GIS technology has a good effect in the collection and processing of land resource information and can effectively improve the management efficiency of land resources.

Data Availability

The labeled dataset used to support the findings of this study are available from the corresponding author upon request.

Conflicts of Interest

The authors declare no competing interests.

Acknowledgments

This study is sponsored by the National Social Science Foundation Project "The Research on Social Capital, CEO Power and Enterprise Resource Allocation along with its Economic Consequences" (Serial Number: 20CGL011).

References

[1] A. Farahbakhsh and M. A. Forghani, "Sustainable location and route planning with GIS for waste sorting centers, case study: Kerman, Iran," *Waste Management & Research*, vol. 37, no. 3, pp. 287–300, 2019.

[2] K. S. Sahitya and C. Prasad, "Modelling structural interdependent parameters of an urban road network using GIS," *Spatial Information Research*, vol. 28, no. 3, pp. 327–334, 2020.

[3] M. A. Dereli, "Monitoring and prediction of urban expansion using multilayer perceptron neural network by remote sensing and GIS technologies: a case study from Istanbul Metropolitan City," *Fresenius Environmental Bulletin*, vol. 27, no. 12a, pp. 9336–9344, 2018.

[4] T. C. M. Guerreiro, J. Kirner Providelo, C. S. Pitombo, R. Antonio Rodrigues Ramos, and A. N. Rodrigues da Silva, "Data-mining, GIS and multicriteria analysis in a comprehensive method for bicycle network planning and design," *International Journal of Sustainable Transportation*, vol. 12, no. 3, pp. 179–191, 2018.

[5] G. Carpentieri and F. Favo, "The end-use electric energy consumption in urban areas: a GIS-based methodology. An application in the city of Naples," *TeMA-Journal of Land Use, Mobility and Environment*, vol. 10, no. 2, pp. 139–156, 2017.

[6] J. France-Mensah, W. J. O'Brien, N. Khwaja, and L. C. Bussell, "GIS-based visualization of integrated highway maintenance and construction planning: a case study of Fort Worth, Texas," *Visualization in Engineering*, vol. 5, no. 1, pp. 1–17, 2017.

[7] K. A. Baba, D. Lal, and A. Bello, "Application of remote sensing and GIS techniques in urban planning, development and management.(A case study of Allahabad District, India)," *International Journal of Scientific & Engineering Research*, vol. 10, no. 6, pp. 1127–1134, 2019.

[8] S. Teixeira, "Qualitative geographic information systems (GIS): an untapped research approach for social work," *Qualitative Social Work*, vol. 17, no. 1, pp. 9–23, 2018.

[9] E. Khayambashi, "Promoting urban spatial and social development, through strategic planning of GIS," *Socio-Spatial Studies*, vol. 2, no. 4, pp. 66–80, 2018.

[10] G. Lü, M. Batty, J. Strobl, H. Lin, A. X. Zhu, and M. Chen, "Reflections and speculations on the progress in geographic information systems (GIS): a geographic perspective," *International Journal of Geographical Information Science*, vol. 33, no. 2, pp. 346–367, 2019.

[11] T. R. Alrobaee, "Measuring spatial justice indices in the traditional Islamic cities by using GIS, An-Najaf Holy City, Iraq a case study," *Journal of Geoinformatics & Environmental Research*, vol. 2, no. 1, pp. 01–13, 2021.

[12] M. R. Meenar, "Using participatory and mixed-methods approaches in GIS to develop a Place-Based Food Insecurity

and Vulnerability Index[J]," *Environment and Planning A*, vol. 49, no. 5, pp. 1181–1205, 2017.

[13] J. J. Gieseking, "Operating anew: queering GIS with good enough software," *The Canadian Geographer/Le Géographe Canadien*, vol. 62, no. 1, pp. 55–66, 2018.

[14] M. Giannopoulou, A. Roukouni, and K. Lykostratis, "Exploring the benefits of urban green roofs: a GIS approach applied to a Greek city," *CES Working Papers*, vol. 11, no. 1, pp. 55–72, 2019.

[15] A. T. N. Dang and L. Kumar, "Application of remote sensing and GIS-based hydrological modelling for flood risk analysis: a case study of District 8, Ho Chi Minh city, Vietnam," *Geomatics, Natural Hazards and Risk*, vol. 8, no. 2, pp. 1792–1811, 2017.

[16] S. K. Yadav and S. L. Borana, "Monitoring and temporal study of mining area of Jodhpur City using remote sensing and GIS," *International Research Journal of Engineering and Technology (IRJET)*, vol. 4, no. 10, pp. 1732–1736, 2017.

[17] W. Chen, G. Zhai, C. Fan, W. Jin, and Y. Xie, "A planning framework based on system theory and GIS for urban emergency shelter system: a case of Guangzhou, China," *Human and Ecological Risk Assessment: An International Journal*, vol. 23, no. 3, pp. 441–456, 2017.

[18] S. Abdullahi and B. Pradhan, "Land use change modeling and the effect of compact city paradigms: integration of GIS-based cellular automata and weights-of-evidence techniques," *Environmental Earth Sciences*, vol. 77, no. 6, pp. 1–15, 2018.

[19] N. Alghais and D. Pullar, "Modelling future impacts of urban development in Kuwait with the use of ABM and GIS," *Transactions in GIS*, vol. 22, no. 1, pp. 20–42, 2018.